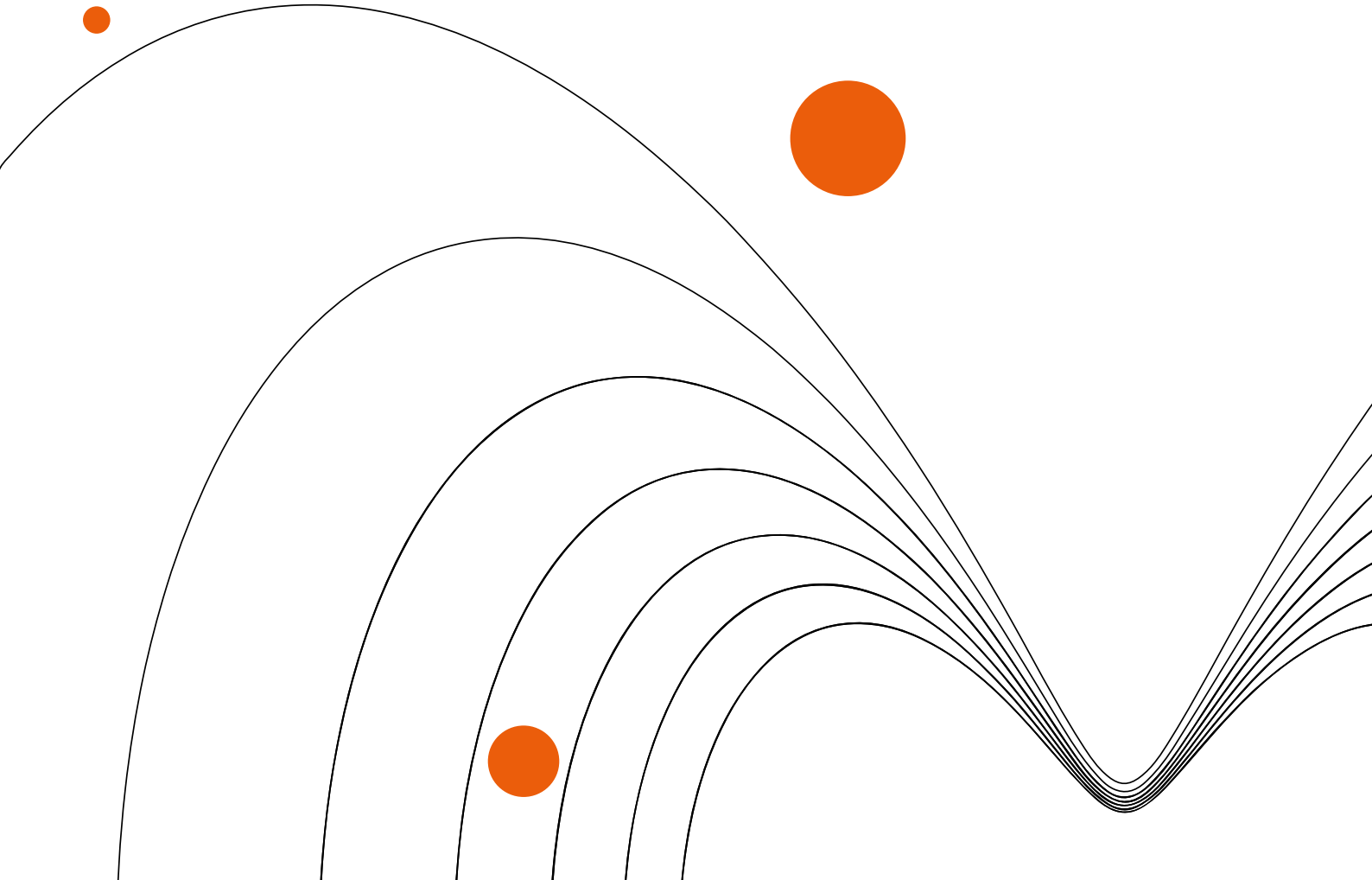
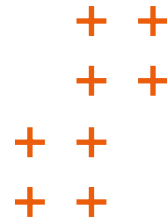




ABSTRACTS

ELI ALPS | 2024





Quantum-optical analysis of high-order harmonic generation in H_2^+ molecules

● J. Rivera-Dean, P. Stammer, A. S. Maxwell, Th. Lamprou, E. Pisanty, P. Tzallas, M. Lewenstein, and M. F. Ciappina

We present a comprehensive theoretical investigation of high-order harmonic generation in H_2^+ molecules within a quantum-optical framework. Our study focuses on characterizing various quantum-optical and quantum-information measures stemming from the correlations established between light and matter. We demonstrate the emergence of entanglement between electron and light states after the laser-matter interaction. We also identify the possibility of obtaining nonclassical states of light in targeted frequency modes by conditioning on specific electronic quantum states, which turn out to be crucial in the generation of highly nonclassical entangled states between distinct sets of harmonic modes. Our findings open up avenues for studying strong-laser-field-driven interactions in molecular systems under a fully quantum-mechanical framework.

SeSo

Paraskevas TZALLAS

Physical Review
A 109 (2024) 033706





Nonclassical states of light after high-harmonic generation in semiconductors: A Bloch-based perspective

● J. Rivera-Dean, P. Stammer, A. S. Maxwell, Th. Lamprou, A. F. Ordóñez, E. Pisanty, P. Tzallas, M. Lewenstein, and M. F. Ciappina

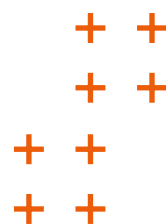
High-harmonic generation (HHG) has emerged as a pivotal process in strong-field physics, yielding extreme ultraviolet radiation and attosecond pulses for a wide range of applications. Furthermore, its emergent connection with the field of quantum optics has revealed its potential for generating nonclassical states of light. Here, we investigate the process of high-harmonic generation in semiconductors under a quantum optical perspective while using a Bloch-based solid-state description. Through the implementation of quantum operations based on the measurement of high-order harmonics, we demonstrate the generation of nonclassical light states similar to those found when driving atomic systems. These states are characterized using diverse quantum optical observables and quantum information measures, showing the influence of electron dynamics on their properties. Additionally, we analyze the dependence of their features on solid characteristics such as the dephasing time and crystal orientation, while also assessing their sensitivity to changes in driving field strength. This paper provides insights into HHG in semiconductors and its potential for generating nonclassical light sources.

SeSo

Paraskevas TZALLAS

Physical Review
B 109 (2024) 035203





Wave packet dynamics and control in excited states of molecular nitrogen

- M. Fushitani, H. Fujise, A. Hishikawa, D. You, S. Saito, Y. Luo, K. Ueda, H. Ibrahim, F. Légaré, S. T. Pratt, P. Eng-Johnsson, J. Mauritsson, A. Olofsson, J. Peschel, E. R. Simpson, P. A. Carpeggiani, D. Ertel, P. K. Maroju, M. Moioli, G. Sansone, R. Shah, T. Csizmadia, M. Dumergue, H. N. Gopalakrishna, S. Kühn, C. Callegari, M. Danailov, A. Demidovich, L. Raimondi, M. Zangrando, G. De Ninno, M. Di Fraia, L. Giannessi, O. Plekan, P. Rebernik Ribic, and K. C. Prince

Wave packet interferometry with vacuum ultraviolet light has been used to probe a complex region of the electronic spectrum of molecular nitrogen, N_2 . Wave packets of Rydberg and valence states were excited by using double pulses of vacuum ultraviolet (VUV), free-electron-laser (FEL) light. These wave packets were composed of contributions from multiple electronic states with a moderate principal quantum number ($n \sim 4-9$) and a range of vibrational and rotational quantum numbers. The phase relationship of the two FEL pulses varied in time, but as demonstrated previously, a shot-by-shot analysis allows the spectra to be sorted according to the phase between the two pulses. The wave packets were probed by angle-resolved photoionization using an infrared pulse with a variable delay after the pair of excitation pulses. The photoelectron branching fractions and angular distributions display oscillations that depend on both the time delays and the relative phases of the VUV pulses. The combination of frequency, time delay, and phase selection provides significant control over the ionization process and ultimately improves the ability to analyze and assign complex molecular spectra.

SeSo

Tamás CSIZMADIA
Mathieu DUMERGUE
Harshitha N. GOPALAKRISHNA
Sergei KÜHN

J. Chem. Phys.
160 (2024) 104203





Tunable ultrafast thermionic emission from femtosecond-laser hot spot on a metal surface by control of laser polarization and angle of incidence: A numerical investigation

● M. Upadhyay Kahaly, S. Madas, B. Mesits, and S. Kahaly

Ultrafast laser induced thermionic emission from metal surfaces has several applications. Here, we investigate the role of laser polarization and angle of incidence on the ultrafast thermionic emission process from laser driven gold coated glass surface. The spatio-temporal evolution of electron and lattice temperatures are obtained using an improved three-dimensional (3D) two-temperature model (TTM) which takes into account the 3D laser pulse profile focused obliquely onto the surface. The associated thermionic emission features are described through the modified Richardson-Dushman equation, including dynamic space-charge effects and are included self-consistently in our numerical approach. We show that temperature-dependent reflectivity influences laser energy absorption. The resulting peak electron temperature on the metal surface monotonically increases with the angle of incidence for the P polarization, while for the S polarization it shows the opposite trend. We observe that thermionic emission duration shows a strong dependence on the angle of incidence and contrasting polarization dependent behavior. The duration of the thermionic current shows strong correlation to the intrinsic electron-lattice thermalization time, in a fluence regime well below the damage threshold of gold. The observations and insights have important consequences in designing ultrafast thermionic emitters using a metal based architecture.

Seso, UFS

**Mousumi UPADHYAY KAHALY
Saibabu MADAS
Subhendu KAHALY**

**Applied Surface Science
643 (2024) 158668**





Atomic ordered doping leads to enhanced sensitivity of phosgene gas detection in graphene nanoribbon: a quantum DFT approach

● R. Deji, G. N. Nagy, B. C. Choudhary, R. K. Sharma, M. K. Kashyap, and M. Upadhyay Kahaly

We explore a novel sensor for detection of phosgene gas by graphene derivatives such as pristine and doped graphene nanoribbons via first principles calculations. The interaction of phosgene molecule with various edge and center doped configurations of boron, phosphorus and boron-phosphorus co-doped armchair graphene nanoribbon (AGNR) and zigzag graphene nanoribbon (ZGNR) is investigated through density functional theory (DFT). P-doped systems showcase chemisorption, displaying enhanced sensitivity to phosgene detection as reflected by a more negative adsorption energy values, accompanied by a prominent charge transfer due to the doping. Regardless of nanoribbon geometry, the binding energies of P-doped systems exhibit notable uniformity within the range of -8.01 eV to -8.49 eV, however the adsorption energies in ZGNR are significantly lower than those observed in AGNR. Due to much higher(lower) electron-donating (accepting) capacity of phosphorous(boron) atoms in comparison to 'C' atom, substitutional doping with 'P' or 'B' atoms in AGNR has significant impact on the structural, electronic and adsorption properties of the nanoribbons. We observe that phosphorus doped configurations (edge/center) effectively interact with phosgene molecule with higher adsorption that corresponds to the chemisorption phenomenon. The strongest adsorption energy (-8.83 eV) is obtained for P doped configurations, followed by that for B+P co-doped AGNR (-4.23 eV). These results suggest significantly stronger adsorption of phosgene gas on P doped AGNR than on any other systems reported so far. Band structure analysis estimates that by phosphorus doping, changes in the band gap is significant and it also shows prominent changes in the band structures. Isosurface electronic charge density plots identify that the transfer of charge takes place from graphene system to phosgene molecule. Thus, significant variation in adsorption and electronic properties of P doped AGNR reveal that these geometries immensely promote the detection of phosgene gas, and may be considered as promising chemical sensor for phosgene removal.

UFS

R Deji RANI
Gergely N. NAGY
Mousumi UPADHYAY
KAHALY

Physica Scripta
99 (2024)3, 035931





Magnetically reconfigurable toroidal metasurfaces

● N. Acharyya, S. Mallick, S. Rane, M. Upadhyay Kahaly, D. R. Chowdhury

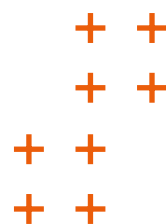
Harnessing electron spin within limited dimensions under applied magnetic fields can lead to spin-assisted tunable light-matter interactions, which form a crucial step in developing frequency-agile opto-spintronic structures toward next generation photonic devices. For this purpose, spin-dependent magneto transport phenomena derived from ferromagnetic (FM)/nonmagnetic (NM) multilayer structures have recently emerged as a useful tool for dynamically tailoring electromagnetic waves. With this pretext, five layers of aluminum (Al)/nickel (Ni) based multilayer thin films in sub skin depth regime are studied in terahertz domain under low-intensity (0 to 30 mT) magnetic fields while systematically varying the NM spacer layer (sandwiched between the FM layers) from 8 to 18 nm. Such thin multi-layer films demonstrate conductivity variations up to $\approx 40\%$ for 30 mT of applied field. Utilizing the same multilayer configurations, magnetic field induced tunability in a metasurface design is investigated that simultaneously manifests toroidal, dipolar, and other higher-order modes. Further, multipolar analysis reveals that the nonradiative toroidal and radiative dipole modes can be enhanced by almost 56% and 183%, respectively, under 0–30 mT magnetic fields. Such magnetic field-induced simultaneous control over radiative and non-radiative resonances can be pivotal for next generation terahertz magnetophotonic devices.

UFS

Mousumi UPADHYAY KAHALY

Advanced Optical Materials





Light-induced photodissociation in the lowest three electronic states of the NaH molecule

● O. Umarov, A. Csehi, P. Badankó, G. J. Halász, and Á. Vibók

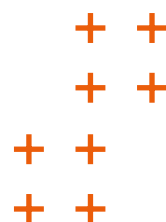
It has been known that electronic conical intersections in a molecular system can also be created by laser light even in diatomics. The direct consequence of these light-induced degeneracies is the appearance of a strong mixing between the electronic and vibrational motions, which has a strong fingerprint on the ultrafast nuclear dynamics. In the present work, pump and probe numerical simulations are performed with the NaH molecule involving the first three singlet electronic states ($X^1\Sigma^+(X)$, $A^1\Sigma^+(A)$ and $B^1\Pi(B)$) and several light-induced degeneracies in the numerical description. To demonstrate the impact of the multiple light-induced non-adiabatic effects together with the molecular rotation on the dynamical properties of the molecule, the dissociation probabilities, kinetic energy release spectra (KER) and the angular distributions of the photofragments were calculated by discussing the role of the permanent dipole moment as well.

UFS

Ágnes VIBÓK

Phys. Chem. Chem. Phys.
26 (2024) 7211-7223





Classical and quantum light-induced non-adiabaticity in molecular systems

● Cs. Fábri, G. J. Halász, L. S. Cederbaum, and Á. Vibók

The exchange of energy between electronic and nuclear motion is the origin of non-adiabaticity and plays an important role in many molecular phenomena and processes. Conical intersections (CIs) of different electronic potential energy surfaces lead to the most singular non-adiabaticity and have been intensely investigated. The coupling of light and matter induces conical intersections, which are termed light-induced conical intersections (LICIs). There are two kinds of LICIs, those induced by classical (laser) light and those by quantum light like that provided by a cavity. The present work reviews the subject of LICIs, discussing the achievements made so far. Particular attention is paid to comparing classical and quantum LICIs, their similarities and differences and their relationship to naturally occurring CIs. In contrast to natural CIs, the properties of which are dictated by nature, the properties of their light-induced counterparts are controllable by choosing the frequency and intensity (or coupling to the cavity) of the external light source. This opens the door to inducing and manipulating various kinds of non-adiabatic effects. Several examples of diatomic and polyatomic molecules are presented covering both dynamics and spectroscopy. The computational methods employed are discussed as well. To our opinion, the young field of LICIs and their impact shows much future potential.

UFS

Ágnes VIBÓK

AVS Quantum Sci.
6 (2024) 2, 023501





Competition of multiphoton ionization pathways in lithium

● B. Tóth, A. Tóth, and A. Csehi

We study the three-photon ionization of atomic lithium by intense, short light pulses, via numerically solving the time-dependent Schrödinger equation. Two-photon Rabi oscillations are induced between the 2s and 4s states, which are damped due to single-photon ionization to the p continuum. Developing a minimal three-level model, we analyze the spectral features of the Autler–Townes (AT) doublet that is formed upon the resonant coupling with the laser pulse. Furthermore, we show that this $2s \rightarrow 4s \rightarrow p$ continuum pathway is the dominant process, if the duration of the laser pulse exceeds a certain value. For shorter pulses, ionization through the 2p state ($2s \rightarrow 2p \rightarrow 4d \rightarrow f$ continuum) gradually becomes the dominant process, provided that the pulse is strong enough to induce several Rabi floppings. Here, we trace the competition of these ionization pathways by observing the structural changes in the shape of the AT doublet.

UFS

Attila TÓTH

J. Phys. B: At. Mol. Opt. Phys.
57 (2024) 055002





Proposal for an electromagnetic mass formula for the X17 particle

● S. Varró

Recent observations of anomalous angular correlations of electron–positron pairs in several nuclear reactions have indicated the existence of a hypothetical neutral boson of rest mass $\sim 17 \text{ MeV}/c^2$, called the X17 particle. Similarly, one has interpreted an independent set of experiments on photon pair spectra around the invariant mass $\sim 38 \text{ MeV}/c^2$, by assuming the existence of the so-called E38 particle. In the present paper, we derive analytical mass formulas for the X17 particle and the E38 particle, on the basis of quantum electrodynamics. We shall use the exact solutions of the Dirac equation of the joint system of a charged particle and plane waves of the quantized electromagnetic radiation. When these solutions are applied to a proton, they lead to dressed radiation quanta with a rest mass of $17.0087 \text{ MeV}/c^2$, which may be identified with the X17 vector bosons. A similar consideration, applied to the odd quarks of the neutron, yields dressed quanta, whose mass equals $37.9938 \text{ MeV}/c^2$, corresponding to the E38 particle. These formulas, besides the Sommerfeld fine structure constant and the masses of the nucleons, do not contain any adjustable parameters. The present analysis also delivers the value 0.846299 fm for the proton radius.

UFS

Sándor VARRÓ

Universe
10 (2024) 2, 86





Survival benefit of stereotactic radiotherapy in the complex management of metastatic melanoma

- Gy. Kelemen, Zs. Együd, Á. Dobi, L. Varga, R. Kószó, E. Borzási, V. Paczona, Z. Végváry, F. Borzák, E. Fodor, H. Ócsai, E. Baltás, J. Oláh, and K. Hideghéty

Background/Aim: Targeted therapy and immunotherapy, with additional stereotactic radiation therapy (SRT) have revolutionized the management of metastatic malignant melanoma (mMM). We aimed to analyze the effectiveness and safety of SRT and determine its role in the complex management of mMM. Patients and Methods: We treated 24 patients with solitary metastasis, 15 with oligometastatic disease and one with multiple metastases. The primary endpoint was to investigate the possible effect of stereotactic radiotherapy for metastatic lesions on patients' survival taking the systemic therapy into consideration. Results: The median overall survival (OS) for the entire group was 30.07 months; 50% of them received immunotherapy, 32% received targeted therapy. Complete remission of the irradiated lesions was observed in six patients, partial tumor response was achieved in 13, while stable disease was detected in 10; tumor progression occurred in four cases. Compartmental recurrence (recurrence in the brain in a not previously irradiated region) developed in seven patients. OS was significantly longer in those with extracranial metastases treated with stereotactic body radiotherapy in comparison to brain SRT. We found a strong correlation between tumor response and mean OS (42.5 months after complete or partial remission versus 11.8 months in those with stable or progressive disease). No OS difference was observed according to the number of irradiated lesions or type of systemic therapy before SRT (no therapy: 43.6 months, with therapy: 25.7 months). Significant OS advantage was shown when immunotherapy was administered post-SRT (mean OS: with immunotherapy: 39.6 months, no immunotherapy: 18.5 months). Conclusion: In the case of oligometastatic MM, SRT can be used safely and with good efficiency in addition to targeted therapy/anti-programmed cell death protein 1 therapy. Improved survival warrants including SRT in the complex management of mMM, however, further studies are needed for SRT optimization.

UFS

Katalin HIDEGHÉTY

Anticancer Research
44 (2024) 1, 205-212





Few-cycle surface plasmon polaritons

- K. Komatsu, Zs. Pápa, T. Jauk, F. Bernecker, L. Tóth, F. Lackner, W. E. Ernst, H. Ditlbacher, J. R. Krenn, M. Ossiander, P. Dombi, and M. Schultze

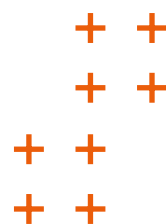
Surface plasmon polaritons (SPPs) can confine and guide light in nanometer volumes and are ideal tools for achieving electric field enhancement and the construction of nanophotonic circuitry. The realization of the highest field strengths and fastest switching requires confinement also in the temporal domain. Here, we demonstrate a tapered plasmonic waveguide with an optimized grating structure that supports few-cycle surface plasmon polaritons with >70 THz bandwidth while achieving >50% light-field-to-plasmon coupling efficiency. This enables us to observe the—to our knowledge—shortest reported SPP wavepackets. Using time-resolved photoelectron microscopy with suboptical-wavelength spatial and sub-10 fs temporal resolution, we provide full spatiotemporal imaging of co- and counter-propagating few-cycle SPP wavepackets along tapered plasmonic waveguides. By comparing their propagation, we track the evolution of the laser-plasmon phase, which can be controlled via the coupling conditions.

UFS

Zsuzsanna PÁPA
László TÓTH
Péter DOMBI

Nano Lett.
24 (2024) 8, 2637–2642





Pt/MnO interface induced defects for high reverse water gas shift activity

- I. Szentı, A. Efremova, J. Kiss, A. Sápi, L. Óvári, Gy. Halasi, U. Haselmann, Z. Zhang, J. Morales-Vidal, K. Baán, Á. Kukovecz, N. López, Z. Kónya

The implementation of supported metal catalysts heavily relies on the synergistic interactions between metal nanoparticles and the material they are dispersed on. It is clear that interfacial perimeter sites have outstanding skills for turning catalytic reactions over, however, high activity and selectivity of the designed interface-induced metal distortion can also obtain catalysts for the most crucial industrial processes as evidenced in this paper. Herein, the beneficial synergy established between designed Pt nanoparticles and MnO in the course of the reverse water gas shift (RWGS) reaction resulted in a Pt/MnO catalyst having ≈ 10 times higher activity compared to the reference Pt/SBA-15 catalyst with $>99\%$ CO selectivity. Under activation, a crystal assembly through the metallic Pt (110) and MnO evolved, where the plane distance differences caused a mismatched-row structure in softer Pt nanoparticles, which was identified by microscopic and surface-sensitive spectroscopic characterizations combined with density functional theory simulations. The generated edge dislocations caused the Pt lattice expansion which led to the weakening of the Pt–CO bond. Even though MnO also exhibited an adverse effect on Pt by lowering the number of exposed metal sites, rapid desorption of the linearly adsorbed CO species governed the performance of the Pt/MnO in the RWGS.

UFS

László ÓVÁRI
Gyula HALASI

Angew. Chem.Int. Ed.
63 (2024) e2023173





Effect of single-crystal TiO_2 /perovskite band alignment on the kinetics of electron extraction

● X. Chen, H. P. Pasanen, R. Khan, N. T. Tkachenko, Cs. Janáky, and G. F. Samu

The kinetics of electron extraction at the electron transfer layer/perovskite interface strongly affects the efficiency of a perovskite solar cell. By combining transient absorption and time-resolved photoluminescence spectroscopy, the electron extraction process between $\text{FA}_{0.83}\text{Cs}_{0.17}\text{Pb}(\text{I}_{0.83}\text{Br}_{0.17})_3$ and TiO_2 single crystals with different orientations of (100), (110), and (111) were probed from subpicosecond to several hundred nanoseconds. It was revealed that the band alignment between the constituents influenced the relative electron extraction process. $\text{TiO}_2(100)$ showed the fastest overall and hot electron transfer, owing to the largest conduction band and Fermi level offset compared to $\text{FA}_{0.83}\text{Cs}_{0.17}\text{Pb}(\text{I}_{0.83}\text{Br}_{0.17})_3$. It was found that an early electron accumulation in these systems can have an influence on the following electron extraction on the several nanosecond time scale. Furthermore, the existence of a potential barrier at the TiO_2 /perovskite interface was also revealed by performing excitation fluence-dependent measurements.

UFS

Csaba JANÁKY
Gergely F. SAMU

J. Phys. Chem. Lett.
15 (2024) 2057–2065





Au-decorated Sb_2Se_3 photocathodes for solar-driven CO_2 reduction

● J. M. Ch. M. Dela Cruz, Á. Balog, P. S. Tóth, G. Bencsik, G. F. Samu, and Cs. Janáky

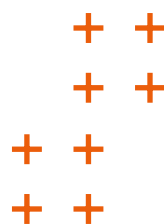
Photoelectrodes with $\text{FTO}/\text{Au}/\text{Sb}_2\text{Se}_3/\text{TiO}_2/\text{Au}$ architecture were studied in photoelectrochemical CO_2 reduction reaction (PEC CO_2RR). The preparation is based on a simple spin coating technique, where nanorod-like structures were obtained for Sb_2Se_3 , as confirmed by SEM images. A thin conformal layer of TiO_2 was coated on the Sb_2Se_3 nanorods via ALD, which acted as both an electron transfer layer and a protective coating. Au nanoparticles were deposited as co-catalysts via photo-assisted electrodeposition at different applied potentials to control their growth and morphology. The use of such architectures has not been explored in CO_2RR yet. The photoelectrochemical performance for CO_2RR was investigated with different Au catalyst loadings. A photocurrent density of $\sim 7.5 \text{ mA cm}^{-2}$ at -0.57 V vs. RHE for syngas generation was achieved, with an average Faradaic efficiency of $25 \pm 6\%$ for CO and $63 \pm 12\%$ for H_2 . The presented results point toward the use of Sb_2Se_3 -based photoelectrodes in solar CO_2 conversion applications.

UFS

Gergely F. SAMU
Csaba JANÁKY

EES. Catal.
2 (2024) 664-674





Temperature dependent carrier dynamics in Ga-alloyed CdSe/ZnS core–shell quantum dots

● K. Sárosi, Ch. Tuinenga, G. F. Samu, K. Mogyorósi, J. Dudás, B. Tóth, P. Jójárt, B. Gilicze, I. Seres, Zs. Bengery, Cs. Janáky, and V. Chikán

In this work, temperature dependent transient absorption spectroscopy measurements are presented on gallium-alloyed CdSe/ZnS core–shell nanoparticles between 30 and 130 °C. To our knowledge, temperature dependent measurements in these systems have been reported only in a few papers, although all processes related to carrier recombination are affected by temperature. For these experiments, gallium-alloyed CdSe/ZnS QD samples were used with nominal doping percentages of 2.5%, 7.5%, 15%. The experimental results show that the transient absorption decay is faster for the pristine CdSe/ZnS samples than in the gallium-alloyed samples at all temperatures. It is assumed that Ga-alloying promotes the formation of trions in the samples by introducing occupied impurity levels within the bandgap of CdSe. The resulting Coulomb blockade will, in turn, prolong the hot-electron relaxation process. By variation of the temperature, the distribution of charge carriers in the different recombination channels can be altered to accelerate recombination in the Ga-alloyed samples at higher temperatures. These measurements demonstrated their usefulness for observing the redistribution of charge carriers among different relaxation pathways.

LaSo, UFS

Krisztina SÁROSI
Gergely F. SAMU
Károly MOGYORÓSI
Júlia DUDÁS
Bálint TÓTH
Péter JÓJÁRT
Barnabás GILICZE
Imre SERES
Zsolt BENERY
Csaba JANÁKY
Viktor CHIKÁN

J. Phys. Chem.
C 128 (2024) 9, 3815–3823

